

Microarcsecond Astrometry with MCAO Using a Diffractive Mask

S. Mark Ammons,¹ Eduardo A. Bendek,² Olivier Guyon,^{2,3}
Bruce Macintosh,¹ and Dmitry Savransky¹

¹Lawrence Livermore National Laboratory
Physics Division L-210
7000 East Ave., Livermore, CA 94550
email: ammons1@llnl.gov

²University of Arizona

³National Astronomical Observatory of Japan, Subaru Telescope

Abstract. We present a new ground-based technique to detect or follow-up long-period, potentially habitable exoplanets via precise relative astrometry of host stars using Multi-Conjugate Adaptive Optics (MCAO) on 8 meter telescopes equipped with diffractive masks. MCAO improves relative astrometry both by cancellation of high-altitude atmospheric layers, which induce dynamic focal-plane distortions, and the improvement of centroiding precision with sharper PSFs. However, mass determination of habitable exoplanets requires multi-year reference grid stability of $\sim 1 - 10 \mu\text{as}$ or nanometer-level stability on the long-term average of out-of-pupil phase errors, which is difficult to achieve with MCAO (e.g., Meyer *et al.* 2011). The diffractive pupil technique calibrates dynamic distortion via extended diffraction spikes generated by a dotted primary mirror, which are referenced against a grid of background stars (Guyon *et al.* 2012). The diffractive grid provides three benefits to relative astrometry: (1) increased dynamic range, permitting observation of $V < 10$ stars without saturation; (2) calibration of dynamic distortion; and (3) a spectrum of the target star, which can be used to calibrate the magnitude of differential atmospheric refraction to the microarcsecond level. A diffractive 8-meter telescope with diffraction-limited MCAO in K-band reaches $< 3 - 5 \mu\text{as}$ relative astrometric error per coordinate perpendicular to the zenith vector in one hour on a bright target star in fields of moderate stellar density ($\sim 10 - 40 \text{ stars arcmin}^{-2}$). We present preliminary on-sky results of a test of the diffractive mask on the Nickel telescope at Lick Observatory.

Keywords. astrometry, techniques:high angular resolution, instrumentation: adaptive optics, stars: planetary systems

1. Introduction

1.1. Science with Microarcsecond Astrometry

The theoretical limits of astrometric precision are orders of magnitude better than what is currently possible (Sozzetti 2010). Robust microarcsecond relative astrometry would be a fundamentally new tool that could be applied to a range of science areas: Earth and exoplanet detection and characterization, Galactic and halo structure, the physics of supermassive black holes and accretion, and stellar astrophysics.

Astrometry is complementary to Doppler and direct imaging techniques for characterizing exoplanets. Both the astrometric signature of an orbiting exoplanet and the contrast-limited sensitivity of direct imaging increase with the separation of the planet from its host star. Thus, astrometry and direct imaging combine to yield full orbit parameters and exoplanet masses with significant overlap between samples (Shao *et al.* 2010, Guyon *et al.* 2012). Astrometry is complementary to radial velocity techniques, which are

more sensitive to planets close to the host star (Unwin *et al.* 2008), and combining the two measurements breaks the $\sin i$ ambiguity, revealing companion mass. Astrometry may be advantageous for following-up exoplanet discoveries made with direct imaging surveys, like the Gemini Planet Imager Exoplanet Survey (GPIES, Macintosh *et al.* 2012), which target young stars that may have significant astrophysical velocity jitter (Figure 1).

Astrometry also compares favorably with Doppler techniques for finding wide-orbit earth-mass exoplanets ($P > 1$ year) around nearby, low-mass M dwarfs or brown dwarfs that require infrared observations (Shao *et al.* 2009). Planetary companions around M stars are being routinely found (e.g., Haghhighipour *et al.* 2010, Johnson *et al.* 2012, Anglada-Escudé *et al.* 2012b) and astrometry is now being used to constrain orbital dynamics (e.g., Dupuy *et al.* 2010, Dupuy & Liu 2012, Anglada-Escudé 2012a).

Combined with radial velocities, microarcsecond astrometry would yield the 3D position and space motions of individual red giants in the Galactic halo, which could constrain models of Galactic structure and the distribution of dark matter within our Galaxy and in local dwarf galaxies (Majewski *et al.* 2009). Beyond our Galaxy, precise astrometry can probe the time variability of the photocenters of nearby quasars and Active Galactic Nuclei (AGN), potentially revealing the space density of binary supermassive black holes and constraining models of the morphology and cloud distribution within the compact optical emission in their central engines (Wehrle *et al.* 2009).

1.2. Astrometry is Limited by Systematic Errors

Much improvement in relative astrometric precision has been realized over the past two decades, particularly as space telescopes and new ground-based techniques like adaptive optics have been exploited. Single-epoch relative precision of 0.1 – 1.0 milliarcseconds is now routine (Pravdo & Shaklan 1996, Benedict *et al.* 1999, Cameron *et al.* 2009, Lu *et al.* 2009).

From the ground, astrometric precision is determined by multiple random error sources that decrease with the square root of exposure time (S/N of star detection and Differential Tip/Tilt Jitter). Long exposures average these errors to reveal noise floors at the $\sim 100 \mu\text{s}$ level (Lu *et al.* 2010). However, the theoretical limits of astrometric precision

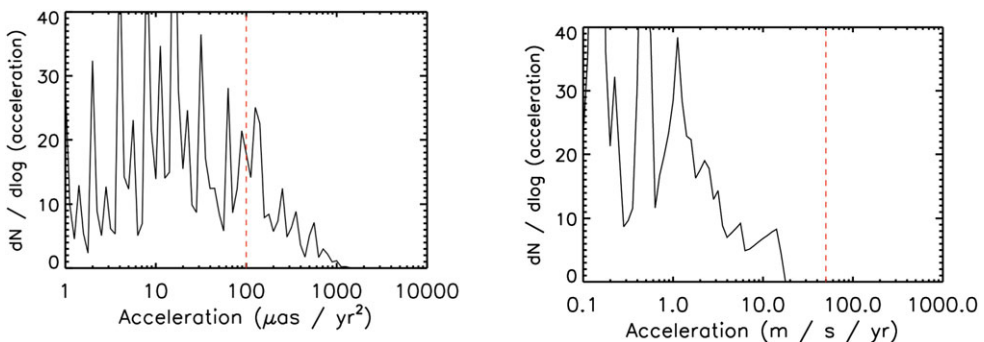


Figure 1. *Left panel:* Histogram of astrometric star acceleration for simulated suite of planetary orbits consistent with detection by the Gemini Planet Imager, with units in $\mu\text{as year}^{-2}$. The red dashed line marks approximately the single-epoch relative astrometric precision obtainable with the best current techniques (Lu *et al.* 2010). A substantial fraction of the detected population has acceleration measurable with astrometric techniques. *Right panel:* Histogram of Doppler star acceleration for the same simulated suite of planetary orbits, with units in $\text{m s}^{-1} \text{ year}^{-1}$. The red dashed line marks the acceleration detectable in one year using Doppler techniques, assuming 50 m s^{-1} astrophysical jitter, as expected for young, active stars. Reproduced from Ammons *et al.* (2012)

improve drastically as telescope diameter increases, and 8 – 30 meter telescopes are predicted to deliver theoretical best precisions of $\sim 1 - 10 \mu\text{s}$ if systematic errors can be addressed (Fritz *et al.* 2010, Trippe *et al.* 2010, Ammons *et al.* 2011, 2012), between one and two orders of magnitude better than what is currently possible (Figure 2). Current astrometric precision appears to be limited by systematic errors like dynamic optical distortion, atmospheric refraction, PSF crowding, etc. (Cameron *et al.* 2009, Sozzetti 2010).

2. Theoretical Limits of Astrometric Precision with MCAO and the Diffractive Pupil

2.1. The Diffractive Pupil Reduces Systematic Astrometric Noise Floors

One potential source of systematic noise floors in astrometry is changing optical distortion, an effect that is expected to be important for space-based platforms (Guyon *et al.* 2011). The *diffractive pupil* concept has been proposed to calibrate changing optical distortion by injecting diffraction spikes into the optical system that trace distortion simultaneously with observations (Guyon *et al.* 2011, Bendek *et al.* 2012, Ammons *et al.* 2012). Three critical advantages of the diffractive pupil concept are that it:

(a) increases dynamic range, permitting observation of $V < 10$ stars without saturation, as the target star astrometry is referenced through diffraction spikes at a significantly lower surface brightness;

(b) maps optical distortion during observations, reducing astrometric errors due to changes in distortion maps from epoch-to-epoch; and

(c) provides a spectrum of the target star, which can theoretically be used to calibrate Differential Atmospheric Refraction (DAR).

2.2. Advantages of MCAO for Astrometry

Multi-Conjugate Adaptive Optics (MCAO) systems achieve diffraction-limited fields of view of 1 – 2 arcminutes by using multiple deformable mirrors to compensate for a 3D volume of turbulence above a telescope. MCAO systems promise multiple potential benefits for astrometry by:

(a) actively canceling upper altitude layers of turbulence, reducing the Differential Tip/Tilt Jitter (DTTJ) component of astrometric error, and controlling plate scale variation;

(b) providing a wider field of view than traditional AO systems, increasing the number of reference stars;

(c) providing a sharper, diffraction-limited PSF, reducing errors due to finite signal-to-noise of star detection;

(d) delivering a more uniform PSF throughout the field, which is critical for constructing a model PSF and reducing star centroiding errors.

2.3. Combining MCAO and the Diffractive Pupil

Although MCAO has many promising advantages, there are risks associated with actively correcting phase errors out of the pupil; small changes in AO system parameters may change the optical distortion map in the focal plane from epoch to epoch. For this reason, we now consider the marriage of the diffractive pupil concept with an MCAO system. Practically, this may be accomplished by constructing a diffractive grid above the primary of a telescope equipped with MCAO or inserting a smaller version in an imaged pupil upstream of the deformable mirrors. To predict the astrometric performance of this hybrid

system, we use the Cameron *et al.* (2009) technique of Lagrange multipliers to assign weights to reference stars.

We simulate an MCAO system on a variety of telescope diameters with a laser guide star (LGS) constellation analogous to the Gemini GEMS MCAO system (Neichel *et al.* 2012) and construct simulated star fields at a specified Galactic latitude to model reference star grids. We include the DTTJ and star S/N error terms in predicting theoretical limits on the relative star astrometry. For these calculations, we assume a $K = 7$ target star at $b = 20^\circ$ Galactic latitude, a 1 hour exposure, a $2'$ field of view with 40% Strehl in K, and use of the full K-band. We model a diffractive pupil as a grid of crisscrossed straight blades of 1 mm thickness and 4 cm spacing, which scatters 3% of the light from the target star into the diffraction spikes. These simulations do not include systematic noise floors due to dynamic optical wander, as the diffractive pupil is expected to calibrate these changes. Other details about the simulation and the assumptions are in Ammons *et al.* (2012).

The predicted astrometric precision for an MCAO-diffractive pupil hybrid system is shown in Figure 2 as a function of telescope diameter. Performance improves sharply with telescope diameter because (1) the larger aperture averages over larger sections of the atmosphere, reducing DTTJ error, and (2) the diffraction limit improves as λ/D .

3. On-sky Tests of the Diffractive Pupil

Here we present preliminary images from an on-sky test of the diffractive pupil concept at the 1-meter Nickel Telescope at Lick Observatory (Figure 3). For this test, we have designed a diffractive mask composed of crisscrossed carbon-fiber blades glued at intersection points (credit Eduardo Bendek), shown mounted on the telescope in the upper left panel of Figure 3. An unprocessed 5 minute image of 51 Per (04 14 53.9 +48 24

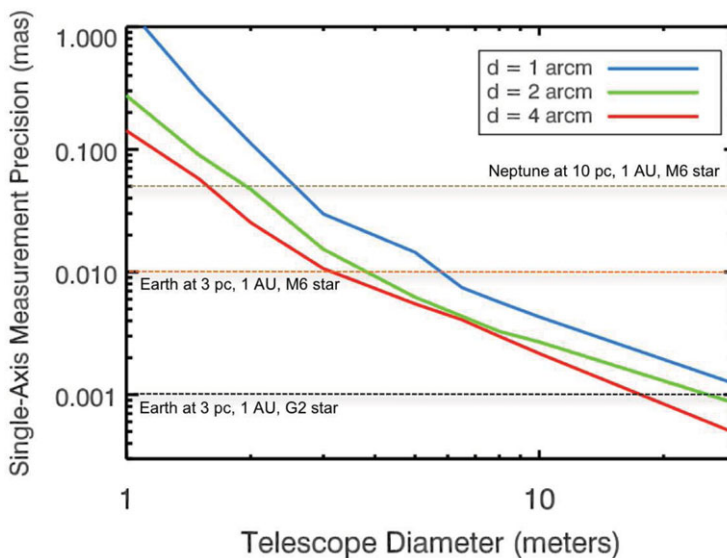


Figure 2. Theoretical limits on single-axis relative astrometric precision in milliarcseconds for MCAO systems as a function of telescope diameter. The simulation assumes a $K = 7$ target star at $b = 20^\circ$, a 1 hour exposure, and a $2'$ field of view with 40% Strehl in K. Colors denote different field diameters. The semi-amplitude astrometric signal is shown for three planet-primary pairs as labeled (assuming circular orbits). Modified from Ammons *et al.* (2012)

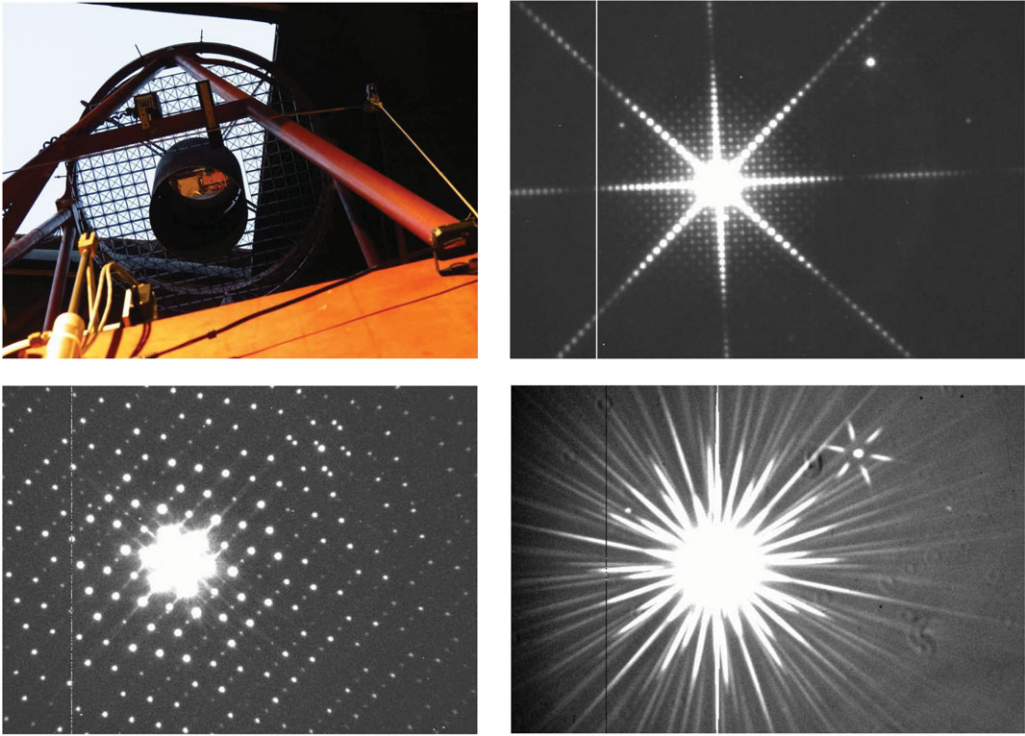


Figure 3. *Upper Left:* An image of the top ring and secondary mirror of the Nickel Telescope with the carbon fiber diffractive mask. *Upper Right:* An unprocessed image of 51 Per taken with a 7630/85 Å narrow-band filter with the Nickel Direct Imager and the carbon fiber diffractive mask. The image was taken Nov 14, 2012. *Lower Left:* A flat-fielded image of 51 Per taken with the perforated aluminum diffractive mask in the 7630/85 Å narrow-band filter on Oct 13, 2012. *Lower Right:* An unprocessed image of 51 Per taken with the perforated aluminum diffractive mask with no filter on Oct 13, 2012. Note that the diffraction spikes appear to curve at the inner edges due to atmospheric refraction when no filter is inserted, as blue optical light is more deflected than red light. All astronomical images have a field of $220'' \times 160''$.

34) taken in a narrow-band filter (7630/85 Å) with the carbon-fiber mask is shown in the upper right panel of Figure 3. Other images of 51 Per are shown taken in the lower panels of Figure 3 with an earlier generation perforated aluminum mask with 9.5 mm hole diameters and 14.3 mm hole spacing in a hexagonal-pack arrangement.

4. Summary

We have calculated the theoretical limits of an MCAO-diffractive pupil hybrid imaging system for ground-based telescopes. The simulations indicate that 8-30 meter class telescopes are capable of achieving 1-10 microarcsecond relative astrometric performance per axis in a single epoch with reasonable exposure times. We have also presented preliminary imaging from an on-sky test of the diffractive pupil at the Nickel 1-meter telescope at Lick Observatory.

5. Acknowledgements

We recognize support from the NASA APRA program. E.A.B. acknowledges support from the Fulbright Science and Technology program. S.M.A. acknowledges research sup-

port from the LLNL Lawrence Fellow program. This work performed under the auspices of the U.S. Department of Energy by Lawrence Livermore National Laboratory under Contract DE-AC52-07NA27344 with document release number LLNL-PROC-565933.

References

- Ammons, S. M., Bendek, E., & Guyon, O. 2011, *proc. SPIE*, 8151, 25
- Ammons, S. M., Bendek, E., Guyon, O., Macintosh, B., & Savransky, D. 2012, *proc. SPIE*, 8447, 0P
- Anglada-Escudé, G., Boss, A., Weinberger, A., Thompson, I., Butler, R., Vogt, S., & Rivera, E. 2012, *ApJ*, 746, 37
- Anglada-Escudé, G., *et al.* 2012, *ApJ*, 751, 16
- Bendek, E., Ammons, S. M., Shankar, H., & Guyon, O. 2011, *proc. SPIE*, 8151, 26
- Benedict, G. F., *et al.* 1999, *AJ*, 118, 1086
- Cameron, P. B., Britton, M., & Kulkarni, S. 2009, *AJ*, 137, 83
- Dupuy, T., Liu, M., Bowler, B., Cushing, M., Helling, C., Witte, S., & Hauschildt, P. 2010, *ApJ*, 721, 1725
- Dupuy, T. & Liu, M. 2012, *ApJ*, 201, 19
- Fritz, T., Gillessen, S., Trippe, S., Ott, T., Bartko, H., Pfuhl, O., Dodds-Eden, K., Davies, R., Eisenhauer, F., & Genzel, R. 2010, *MNRAS*, 401, 1177
- Guyon, O., Bendek, E., Ammons, S. M., Shao, M., Shaklan, S., Woodruff, J., & Belikov, R. 2011, *proc. SPIE*, 8151, 24
- Guyon, O., Bendek, E., Eisner, J., Angel, R., Woolf, N., Milster, T., Ammons, S. M., Shao, M., Shaklan, S., Levine, M., Nemat, B., Pitman, J., Woodruff, J., & Belikov, R. 2012, *ApJS*, 200, 11
- Haghighipour, N., Vogt, S., Butler, R., Rivera, E., Laughlin, G., Meschiar, S., & Henry, G. 2010, *ApJ*, 715, 271
- Johnson, J., *et al.* 2012, *AJ*, 143, 111
- Lu, J., Ghez, A., Yelda, S., Do, T., Clarkson, W., McCrady, N., & Morris, M. 2010, *proc. SPIE*, 7736, 51
- Macintosh, B., Anthony, A., Atwood, J., *et al.* 2012, *proc. SPIE*, 8446, 1U
- Majewski, S., *et al.* 2009, Chapter 4 of *SIM Lite Book*, (arXiv:0902.2759)
- Meyer, E., Kürster, M., Arcidiacono, C., Ragazzoni, R., & Rix, H.-W. 2011, *A&A*, 532, 16
- Neichel, B., *et al.* 2012, *proc. SPIE*, 8447, 4Q
- Pravdo, S. & Shaklan, S. 1996, *ApJ*, 465, 264
- Shao, M., Marcy, G., Catanzarite, J., Edberg, S., Leger, A., Malbet, F., Queloz, D., Muterspaugh, M., Beichman, C., Fischer, D., Ford, E., Olling, R., Kulkarni, S., Unwin, S., & Traub, W. 2009, *astro2010*, 271 (<http://arxiv.org/abs/0904.0965>)
- Shao, M., Catanzarite, J., & Pan, X. 2010, *ApJ*, 720, 357
- Sozzetti, A. 2010, *EAS Publications Series*, 42, 55
- Trippe, S., Davies, R., Eisenhauer, F., Schreiber, N., Fritz, T., & Genzel, R. 2010, *MNRAS*, 402, 1126
- Unwin, S., Shao, M., & Edberg, S. 2008, *proc. SPIE*, 7013, 78
- Wehrle, A., *et al.* 2009, Chapter 11 of *SIM Lite Book*